

Analytic methods for field induced tunneling in quantum wells with arbitrary potential profiles

S PANDA and B K PANDA

Institute of Physics, Sachivalaya Marg, Bhubaneswar 751 005, India
Email: sudhira@iopb.res.in; bpanda@iopb.res.in

MS received 27 September 2000; revised 28 February 2001

Abstract. Electric field induced tunneling is studied in three different types of quantum wells by solving time-independent effective mass equation in analytic methods based on three different Airy function approaches. Comparison of different Airy function methods indicates that they are identical and connected to each other by the Breit–Wigner formula.

Keywords. Quantum wells; Airy function methods; tunneling.

PACS Nos 66.30.Ny; 73.20.Dx; 73.40.Gk

1. Introduction

Quantum wells (QW) formed in the semiconductor heterostructures have been given considerable theoretical attention because of their optical device applications [1]. For understanding the operating principles of devices, it is necessary to study the optical absorption spectra in the QW under an applied dc electric field perpendicular to the growth direction [2]. The intensity of the absorption spectra depends on the dephasing rate and is the combination of the relaxation time due to the electron-phonon scattering and the mean tunneling lifetime of carriers due to the electric field [3]. The electron-phonon mean relaxation time can be determined in a semi-classical picture whereas the mean tunneling lifetime is a complete quantum phenomena [4]. Moreover, the peak position of the absorption spectra is governed by the Stark shifted energy levels, which also need a complete quantum mechanical calculation. The electronic structure of the quantum wells under the electric field has been studied using *ab initio* formalisms [5]. However, in the present work we have employed the effective mass equation [1] for simplicity.

The Stark shifted energy levels in a single rectangular quantum well (RQW) are thoroughly studied using both analytic Airy function methods [6–9] and numerical methods [10–14]. The Airy function methods are also efficient in calculating the mean tunneling lifetimes (τ). Recently Panda *et al* [15] have presented accurate numerical methods based on the Fourier series expansion techniques for calculating τ in quantum wells with arbitrary

form of the potential profile. The analytic method is always preferred for its simplicity and requirement of modest computational facilities.

In the single RQW there are three different Airy function methods available to obtain Stark shifted energies and mean tunneling lifetimes [6–9]. Under the uniform electric field the Stark shifted energy levels and mean tunneling lifetimes are calculated as the resonance position (E_r) and width ($\Gamma = \hbar/\tau$) in the Breit–Wigner formalism [16]. Austin and Jaros [6] have calculated E_r and Γ in the phase shift method. Enderlein *et al* [7] have used the density of states method for calculating E_r and Γ . Ghatak *et al* [8] have presented this method in the spirit of wave mechanics. Ahn and Chuang [9] have expressed E_r and Γ from the single complex energy eigenvalue. The complex energy is obtained using Airy functions with complex arguments. This method has been employed by Peng *et al* [17] in order to calculate E_r and Γ in the symmetric double quantum wells (DQW).

Ghatak *et al* [8] have generalized the real Airy function method to calculate E_r and Γ in the quantum wells with arbitrary form of the potential profile. This is achieved by dividing the potential into a number of small strips, such that the potential in each strip can be approximated by a rectangular barrier. Both E_r and Γ are obtained from the current continuity conditions. Yang *et al* [18] have used this method to calculate E_r and Γ in the annealing induced diffusion modified quantum well (DMQW).

Unfortunately the position dependence of the effective mass has not been taken into account in all Airy function methods presented above. Hutchings [19] has shown that the inclusion of the barrier effective mass has got significant effects on E_r and Γ .

This paper deals with two important aspects of the Airy function methods. (i) We incorporate the position dependence of the effective mass in the current continuity condition for calculating E_r and Γ under electric fields. For achieving this we have followed the work of Hutchings [19]. (ii) We compare three different Airy function methods for reproducing the same results. To the best of our knowledge such a comparison does not exist before. In order to make our methods simple, we have not included strain and non-parabolicity [20] in our calculations. However, the inclusion of these effects in the present Airy function formalisms is rather straightforward.

2. Methods of calculations and results

In this section we describe details of the application of the real and complex Airy function methods for calculating the E_r and Γ in the quantum wells under uniform electric field. The effective mass equation for a given energy E is given by [21]

$$\left[-\frac{\hbar^2}{2} \frac{\partial}{\partial z} \frac{1}{m^*(z)} \frac{\partial}{\partial z} + V(z) + eFz \right] \Psi_E(z) = E\Psi_E(z), \quad (1)$$

where $m^*(z)$ is the position dependent effective mass, $V(z)$ is the confinement potential, e is the magnitude of the electric charge and F is the applied electric field.

The effective mass and the potential profile are constant in a given region. The effect of the electric field is only to change the slope of the potential in that region by the polarity of the applied bias. Therefore eq. (1) for the i th region is expressed as

$$\frac{d^2 \Psi_E^i(z)}{dz^2} - \frac{2m_i}{\hbar^2} (V_i(z) + eFz - E) \Psi_E^i(z) = 0, \quad (2)$$

where $\Psi_E^i(z)$ and m_i are the energy dependent wave function and effective mass respectively for the i th region. We introduce a dimensionless co-ordinate η which is related to z as

$$\eta = - \left[\frac{2m_i}{(e\hbar F)^2} \right]^{1/3} (E - V_i(z) - eFz). \quad (3)$$

Substituting eq. (3) in eq. (2) we find,

$$\frac{d^2 \Psi_E^i(\eta)}{d\eta^2} - \eta \Psi_E^i(\eta) = 0. \quad (4)$$

The solution of eq. (4) is expressed as

$$\Psi_E^i(\eta) = C_i Ai(\eta) + D_i Bi(\eta), \quad (5)$$

where Ai and Bi are Airy functions [22] with coefficients C_i and D_i respectively for the i th region. The required boundary conditions for getting coefficients are obtained from the current continuity conditions at the heterojunction z_0 as [21]

$$\Psi_E^i(z)|_{z=z_0} = \Psi_E^{i+1}(z)|_{z=z_0}, \quad (6a)$$

$$\frac{1}{m_i^*} \frac{d\Psi_E^i(z)}{dz} \Big|_{z=z_0} = \frac{1}{m_{i+1}^*} \frac{d\Psi_E^{i+1}(z)}{dz} \Big|_{z=z_0}. \quad (6b)$$

A. Single rectangular quantum well

The potential profile of this well is given by

$$V(z) = \begin{cases} 0 & \text{for } |z| < l/2; \\ V_0 & \text{for } |z| \geq l/2, \end{cases} \quad (7)$$

where $V_0 = B_{\text{off}}[E_g(x) - E_g(0)]$. $E_g(x)$ and $E_g(0)$ are the band gaps of $\text{Al}_x\text{Ga}_{1-x}\text{As}$ and GaAs respectively. B_{off} is the band offset. In the barrier region ($|z| \geq l/2$) the effective mass of $\text{Al}_x\text{Ga}_{1-x}\text{As}$ is $m^*(x)$ and in the well region ($|z| < l/2$) the effective mass of GaAs is given by $m^*(0)$. The parametrized forms of $E_g(x)$ and $m^*(x)$ are taken from the compiled work of Adachi [23]. The single RQW considered in the present case is shown in figure 1.

The η and $m^*(z)$ are different inside and outside the well region. The wave functions in the well and barrier regions are described as

$$\Psi_E(\eta) = \begin{cases} C_1 Ai(\eta), & z \geq l/2; \\ C_2 Ai(\eta) + D_2 Bi(\eta), & |z| < l/2; \\ C_3 Ai(\eta) + D_3 Bi(\eta), & z \leq -l/2, \end{cases} \quad (8)$$

where C_1, C_2, D_2, C_3 and D_3 are constants. From the properties of Airy functions it is clear that $Bi(\eta)$ increases with increasing η and becomes infinity when η is at infinity.

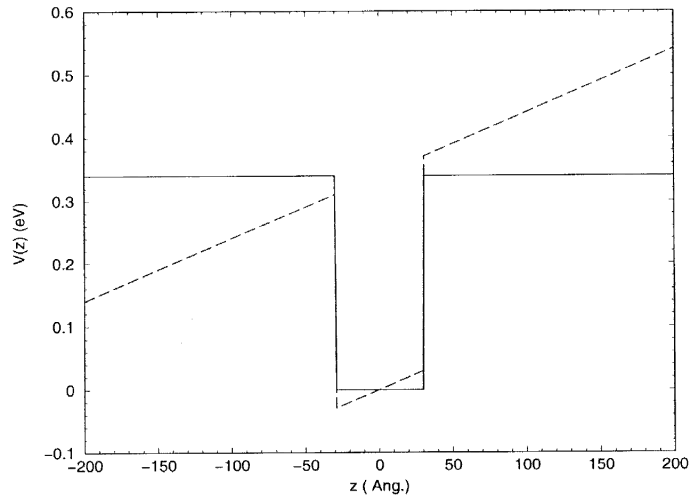


Figure 1. Potential profile of the single rectangular quantum well under the uniform electric field. The electric field strength is 100 kV/cm. In calculating the potential profiles we have taken $x = 0.353$, $l = 100\text{\AA}$ and $B_{\text{off}} = 0.7$. The solid line and the dashed line are the potential before and after the applied electric field, respectively.

In order to make the wave function well behaved in the entire region, this part is not added in the wave function in the region $z \geq l/2$.

2.1 Phase-shift method

The Stark resonances are characterized by a rapid increase of the π in the phase ϕ , where [24]

$$\tan(\phi) = \frac{D_3}{C_3}. \quad (9)$$

In this method E_r and Γ are related to $\tan(\phi)$ in the Breit–Wigner formalism as

$$\tan(\phi) = \frac{\Gamma}{2(E_r - E)}. \quad (10)$$

From eq. (10) we observe that E_r is obtained from the pole of $\tan(\phi)$. From eq. (9), we find that this condition is satisfied when

$$C_3(E_r) = 0. \quad (11)$$

The value of Γ is calculated in the following manner. From eqs (9) and (10) we find that

$$\Gamma = 2(E_r - E) \frac{D_3}{C_3}. \quad (12)$$

Expanding $C_3(E)$ in Taylor’s series, and then using eq. (11) we obtain

$$C_3(E) = C_3(E_r) + (E_r - E)C_3'(E_r) + \dots = (E_r - E)C_3'(E_r), \quad (13)$$

where higher order terms are neglected and $C_3'(E_r) = dC_3(E)/dE|_{E_r}$. Substituting eq. (13) in eq. (12) we find the expression for Γ as

$$\Gamma = 2 \frac{D_3(E_r)}{C_3'(E_r)}. \quad (14)$$

2.2 Density of states method

The method of finding E_r and Γ from the density of states in the Rydberg Stark problem has been formulated by Luc-Koenig and Bachelier [25]. This method has been used in quantum well problems by several groups [7,8,26]. The time-dependent wave function is defined as

$$\Psi(z, t) = \int C(E) \Psi_E(z) e^{-jEt/\hbar}, \quad (15)$$

where $j = \sqrt{-1}$ and $C(E)$ is the normalization constant. The wave function for a state $\Psi(z)$ is obtained as $\Psi(z, t = 0)$. The density of states is the square of the normalization constant which is derived from eq. (15) as [25,26]

$$C^2(E) = \left| \int \Psi(z, t = 0) \Psi_E(z) dz \right|^2. \quad (16)$$

Substitution of eq. (8) in eq. (16) yields $C^2(E)$ as [26,27]

$$C^2(E) = \frac{G}{C_3^2(E) + D_3^2(E)}, \quad (17)$$

where $G = (2m^*(x)eF/\hbar^2)^{1/6} \pi/\sqrt{L}$. In the vicinity of the resonance energy, $C^2(E)$ is given by the Breit-Wigner formula

$$C^2(E) = C^2(E_r) \frac{(\Gamma/2)^2}{(E - E_r)^2 + (\Gamma/2)^2}. \quad (18)$$

E_r is obtained by locating the maximum of $C^2(E)$. Comparing eqs (17) and (18) and using eq. (13), we find that $C_3(E_r) = 0$ and $\Gamma = 2D_3/C_3'$. This method also reproduces eqs (11) and (14) found independently from the phase-shift method.

2.3 Numerical methods for evaluating E_r and Γ

There are two different but similar numerical techniques [7,8,19] to obtain E_r and Γ in the real Airy function methods. The technique followed by Endelein *et al* [7] is described first.

Using the continuity equations (6a) and (6b) at $z = l/2$ and $-l/2$ we obtain four equations which can be arranged as

$$M \begin{pmatrix} C_2 \\ D_2 \\ C_3 \\ D_3 \end{pmatrix} = C_1 \begin{pmatrix} Ai(\eta_b^{+1}) \\ \frac{Ai'(\eta_b^{+1})}{m(x)} \\ 0 \\ 0 \end{pmatrix}, \quad (19)$$

where the matrix M is given by

$$M = \begin{pmatrix} Ai(\eta_a^{+1}) & Bi(\eta_a^{+1}) & 0 & 0 \\ \frac{Ai'(\eta_a^{+1})}{m(0)} & \frac{Bi'(\eta_a^{+1})}{m(0)} & 0 & 0 \\ -Ai(\eta_a^{-1}) & -Bi(\eta_a^{-1}) & Ai(\eta_b^{-1}) & Bi(\eta_b^{-1}) \\ -\frac{Ai'(\eta_a^{-1})}{m(0)} & -\frac{Bi'(\eta_a^{-1})}{m(0)} & \frac{Ai'(\eta_b^{-1})}{m(x)} & \frac{Bi'(\eta_b^{-1})}{m(x)} \end{pmatrix}, \quad (20)$$

where $m(x) = [m^*(x)]^{2/3}$ and $m(0) = [m^*(0)]^{2/3}$ and η values at boundaries $\pm l/2$ are given by

$$\eta_a^{\pm 1} = - \left[\frac{2m^*(0)}{(e\hbar F)^2} \right]^{1/3} \left(E \mp eF \frac{l}{2} \right), \quad (21a)$$

$$\eta_b^{\pm 1} = - \left[\frac{2m^*(x)}{(e\hbar F)^2} \right]^{1/3} \left(E - V_0 \mp eF \frac{l}{2} \right). \quad (21b)$$

The Wronkian determinant of $Ai(\eta)$ and $Bi(\eta)$ is expressed as [22]

$$Ai(\eta)Bi'(\eta) - Ai'(\eta)Bi(\eta) = \frac{1}{\pi}. \quad (22)$$

Using eq. (22), the determinant of the matrix M is obtained as

$$|M| = \frac{1}{\pi^2} \left(\frac{1}{m^*(0)m^*(x)} \right)^{2/3}. \quad (23)$$

Since the $|M|$ is not zero everywhere, eq. (19) may be solved for all values of energy E making the energy spectrum continuous. The coefficients $C_1(E)$, $C_2(E)$, $D_2(E)$, $C_3(E)$ and $D_3(E)$ are uniquely determined in dependence of $C_1(E)$. Since $C_1(E)$ is arbitrary in the normalization constant, it can be taken as unity ($C_1(E) = 1$). The coefficients $C_3(E)$ and $D_3(E)$ are obtained from the following determinants,

$$C_3(E) = \frac{1}{|M|} \begin{bmatrix} Ai(\eta_a^{+1}) & Bi(\eta_a^{+1}) & Ai(\eta_b^{+1}) & 0 \\ \frac{Ai'(\eta_a^{+1})}{m(0)} & \frac{Bi'(\eta_a^{+1})}{m(0)} & \frac{Ai'(\eta_b^{+1})}{m(x)} & 0 \\ -Ai(\eta_a^{-1}) & -Bi(\eta_a^{-1}) & 0 & Bi(\eta_b^{-1}) \\ -\frac{Ai'(\eta_a^{-1})}{m(0)} & -\frac{Bi'(\eta_a^{-1})}{m(0)} & 0 & \frac{Bi'(\eta_b^{-1})}{m(x)} \end{bmatrix}, \quad (24)$$

$$D_3 = \frac{1}{|M|} \begin{bmatrix} Ai(\eta_a^{+1}) & Bi(\eta_a^{+1}) & 0 & Ai(\eta_b^{+1}) \\ \frac{Ai'(\eta_a^{+1})}{m(0)} & \frac{Bi'(\eta_a^{+1})}{m(0)} & 0 & \frac{Ai'(\eta_b^{+1})}{m(x)} \\ -Ai(\eta_a^{-1}) & -Bi(\eta_a^{-1}) & Ai(\eta_b^{-1}) & 0 \\ -\frac{Ai'(\eta_a^{-1})}{m(0)} & -\frac{Bi'(\eta_a^{-1})}{m(0)} & \frac{Ai'(\eta_b^{-1})}{m(x)} & 0 \end{bmatrix}. \quad (25)$$

The roots of the eq. (24) represent (E_r) which are computed by the Newton and Raphson method [28]. For calculating Γ the derivative $C_3'(E_r)$ is calculated in the finite difference scheme by symmetrically varying E_r by a small increment.

The second method for obtaining E_r and Γ is based on the transfer matrix technique [8,19]. As in eq. (19) the continuity equations are used at a boundary to obtain

$$\begin{pmatrix} Ai(\eta_b^{-(i)}) & Bi(\eta_b^{-(i)}) \\ \frac{Ai'(\eta_b^{-(i)})}{m_i^-} & \frac{Bi'(\eta_b^{-(i)})}{m_i^-} \end{pmatrix} \begin{pmatrix} C_{i+1} \\ D_{i+1} \end{pmatrix} = \begin{pmatrix} Ai(\eta_a^{+(i)}) & Bi(\eta_a^{+(i)}) \\ \frac{Ai'(\eta_a^{+(i)})}{m_i^+} & \frac{Bi'(\eta_a^{+(i)})}{m_i^+} \end{pmatrix} \begin{pmatrix} C_i \\ D_i \end{pmatrix}. \quad (26)$$

At $l/2$, we take $C_1(E) = 1$, $D_1(E) = 0$, η_a^{+1} and η_b^{+1} to find $C_2(E)$ and $D_2(E)$ at different E in a given energy range. At $-l/2$, $C_2(E)$, $D_2(E)$, η_a^{-1} and η_b^{-1} are used to find $C_3(E)$ and $D_3(E)$. Then E_r values are obtained from the root of $C_3(E) = 0$. The width Γ is obtained from eq. (14).

2.4 Complex airy function method

Substituting eq. (18) in eq. (15) for a single E_r , $\Psi(z, t)$ is derived as [16]

$$\Psi(z, t) = \Psi(z) e^{-\frac{i}{\hbar}(E_r - \frac{j}{2}\Gamma)t}, \quad (27)$$

where $t \geq 0$. The time-dependent effective mass is given by [1]

$$\left[-\frac{\hbar^2}{2} \frac{\partial}{\partial z} \frac{1}{m^*(z)} \frac{\partial}{\partial z} + V(z) + eFz \right] \Psi(z, t) = j\hbar \frac{\partial}{\partial t} \Psi(z, t). \quad (28)$$

Substituting eq. (27) in eq. (28) we find

$$\left[-\frac{\hbar^2}{2} \frac{\partial}{\partial z} \frac{1}{m^*(z)} \frac{\partial}{\partial z} + V(z) + eFz \right] \Psi(z) = \left(E_r - \frac{j}{2}\Gamma \right) \Psi(z). \quad (29)$$

Ahn and Chuang [9] have used this equation to calculate E_r and Γ . The dimensionless co-ordinate η in this case is defined as

$$\eta = - \left[\frac{2m_i}{(e\hbar F)^2} \right]^{1/3} \left(E - \frac{j}{2}\Gamma - V_i(z) - eFz \right). \quad (30)$$

We find that η is complex in this approach.

Before proceeding to define the wave function in this approach, it is also important to establish the connection between the phase-shift analysis and complex Airy function method. From eqs (9) and (10) we find that

$$C_3 = D_3 \frac{2(E_r - E)}{\Gamma}. \quad (31)$$

In the vicinity of E_r , we obtain

$$C_3 = D_3 \frac{2[E_r - (E_r - \frac{j}{2}\Gamma)]}{\Gamma} = jD_3. \quad (32)$$

Substituting eq. (32) in eq. (8) we obtain,

$$\Psi_E(\eta) = \begin{cases} C_1 Ai(\eta), & z \geq l/2; \\ C_2 Ai(\eta) + D_2 Bi(\eta), & |z| < l/2; \\ D_3 [Bi(\eta) + j Ai(\eta)], & z \leq -l/2. \end{cases} \quad (33)$$

Since η is complex, the Airy functions are required to be evaluated with complex arguments. In the present case we have no opportunity to use eqs (11) and (14) for evaluating E_r and Γ . Using the continuity conditions at $z = \frac{l}{2}$ and $z = -\frac{l}{2}$ we obtain four equations. In order that the coefficients C_1 , C_2 , D_2 and D_3 have non-zero values, the determinant has to be zero,

$$\begin{vmatrix} Ai(\eta_b^{+1}) & -Ai(\eta_a^{+1}) & -Bi(\eta_a^{+1}) & 0 \\ \frac{Ai'(\eta_b^{+1})}{m(x)} & -\frac{Ai'(\eta_a^{+1})}{m(0)} & -\frac{Bi'(\eta_a^{+1})}{m(0)} & 0 \\ 0 & Ai(\eta_a^{-1}) & Bi(\eta_a^{-1}) & -BA(\eta_b^{-1}) \\ 0 & \frac{Ai'(\eta_a^{-1})}{m(0)} & \frac{Bi'(\eta_a^{-1})}{m(0)} & -\frac{BA'(\eta_a^{-1})}{m(x)} \end{vmatrix} = 0. \quad (34)$$

In this equation we have taken $BA(\eta_b^{-1}) = Bi(\eta_b^{-1}) + jAi(\eta_b^{-1})$ and $BA'(\eta_b^{-1}) = Bi'(\eta_b^{-1}) + jAi'(\eta_b^{-1})$. The complex roots of the complex determinant are obtained in the Newton–Raphson method [28].

We have shown E_r and Γ at different field strengths in table 1. Our results are identical in both real Airy and complex Airy function methods. As expected the quasi-bound energies decrease with increasing applied field whereas resonance widths are increased with increasing electric field due to tunneling.

B. Symmetric double quantum well

The Airy function methods are then applied to the symmetric double quantum well (DQW) [29] which is formed by two single RQWs of width (l) separated by a barrier of width h . The potential profile for this well is expressed in the following form:

Table 1. Ground state energies and resonance widths in the single RQW as shown in figure 1 at different applied electric fields.

F (kV/cm)	E_r (eV)	Γ (eV)
50	0.031455	2.574×10^{-23}
100	0.026957	2.110×10^{-11}
150	0.019862	1.585×10^{-7}
200	0.010461	1.217×10^{-5}
250	-0.00094	1.451×10^{-4}

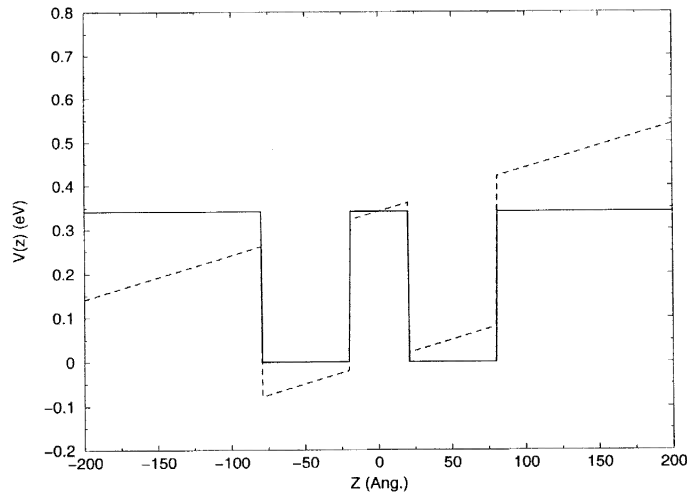


Figure 2. Potential profile of the symmetric double quantum well under the uniform electric field. The electric field strength is 100 kV/cm. In calculating the potential profile we have taken $x = 0.353$, $l = 60\text{\AA}$, $h = 40\text{\AA}$ and $B_{\text{off}} = 0.7$. Notations in this figure are the same as in figure 1.

$$V(z) = \begin{cases} V_0 & \text{for } |z| < h/2; \\ 0 & \text{for } h/2 < |z| < l + h/2; \\ V_0 & \text{for } |z| \geq l + h/2. \end{cases} \quad (35)$$

The potential profile of this well is shown in figure 2. As in eq. (8), the wave function for this well is described as

$$\Psi_E(\eta) = \begin{cases} C_1 Ai(\eta), & z \geq l + h/2; \\ C_2 Ai(\eta) + D_2 Bi(\eta), & h/2 < z < l + h/2; \\ C_3 Ai(\eta) + D_3 Bi(\eta), & |z| < h/2; \\ C_4 Ai(\eta) + D_4 Bi(\eta), & -L/2 < z < -l - h/2; \\ C_5 Ai(\eta) + D_5 Bi(\eta), & z \leq -l - h/2. \end{cases} \quad (36)$$

For the complex Airy function method [17], the wave function for the region $z \leq -l - h/2$ is modified as $D_5[Bi(\eta) + jAi(\eta)]$. The values of η at four boundaries are defined as

$$\eta_a^{\pm 2} = - \left[\frac{2m^*(0)}{(e\hbar F)^2} \right]^{1/3} \left(E \mp eF \left(l + \frac{h}{2} \right) \right), \quad (37a)$$

$$\eta_b^{\pm 2} = - \left[\frac{2m^*(x)}{(e\hbar F)^2} \right]^{1/3} \left(E - V_0 \mp eF \left(l + \frac{h}{2} \right) \right). \quad (37b)$$

The continuity conditions (eq. (6)) at $z = l + h/2$, $h/2$, $-h/2$ and $-l - h/2$ result eight equations in both real and complex Airy function methods. In the real Airy function method, E_T and Γ can be evaluated easily from the equations $C_5(E) = 0$ and

Table 2. Ground state energies and resonant widths in the symmetric DQW shown in figure 2 at different applied electric fields.

F (kV/cm)	E_r (eV)	Γ (eV)
50	0.04113	4.728×10^{-21}
80	0.025409	1.088×10^{-13}
100	0.01482	3.056×10^{-11}
120	0.00403	1.310×10^{-9}
150	-0.012387	5.4789×10^{-8}

$\Gamma = 2D_5(E_r)/C_5'(E_r)$, whereas E_r and Γ are determined from the complex roots of the determinant obtained from the continuity conditions of the wave functions in the complex Airy function method [17].

As in the single RQW, the E_r and Γ in the real and complex Airy function methods are identical at different applied field strengths. We have shown E_r and Γ at different field strengths in table 2. As observed before [15], E_r decreases rapidly with increasing electric field strength, while Γ increases slowly with that due to the barrier present between two single RQWs.

C. Diffusion modified quantum well

When the single RQW is subject to annealing above 800°C, intermixing starts at the heterojunction [30–32]. The formation of the Ga vacancies in the well region induces Al atoms from the barrier to diffuse into the well. The inter-diffusion process is therefore characterized by the Al diffusion length ($L_d = \sqrt{Dt}$) which can be obtained from the diffusion constant (D) at the annealing temperature and the annealing time (t). Khreis, Gillin and Homewood [33] have however, recently found that the concentration of vacancies in the substrate material are responsible for the inter-diffusion process. Thus there is no thermal stability of the heterostructures. With good surface encapsulation it is possible to reduce the background concentration and get a DMQW. Taking the diffusion constant to be isotropic, the position dependent Al concentration from the diffusion equation is found to be [2]

$$w(z) = x \left[1 - \frac{1}{2} \left\{ \operatorname{erf} \left(\frac{l+2z}{4L_d} \right) + \operatorname{erf} \left(\frac{l-2z}{4L_d} \right) \right\} \right], \quad (38)$$

where ‘erf’ is the error function [22] and l is the width of the RQW. The potential profile is expressed as

$$V(z) = B_{\text{off}} [E_g(w(z)) - E_g(w(0))]. \quad (39)$$

The potential profile is shown in figure 3. Unlike in the previous quantum well structures, in the present case there is no boundary between the well and barrier regions. The effective mass varies in the entire quantum well structure. As discussed earlier, the potential profile is subdivided into a number of strips. Before applying electric field the potential within

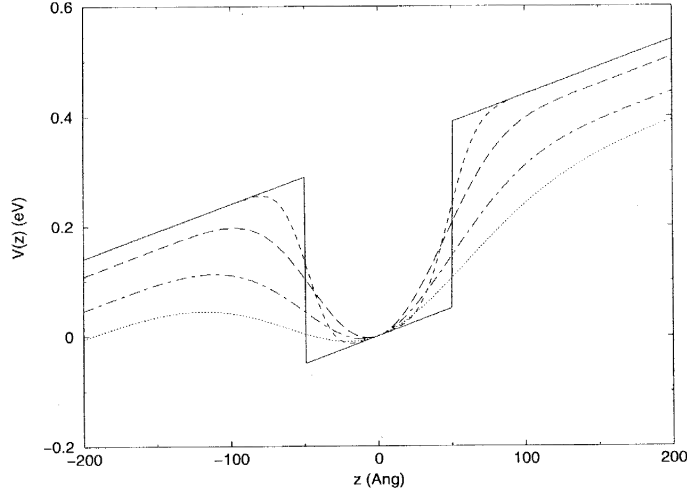


Figure 3. Potential profile of the diffusion modified quantum well under the uniform electric field. The solid, dashed, long-dashed, dot-dashed and dotted lines are the potential profiles calculated at $L_d = 0, 10, 20, 30$ and 40\AA respectively. Parameters in this figure are the same as in figure 1. The potentials in wells for $L_d = 30$ and 40\AA are very shallow. We have presented results for wells at $L_d = 10$ and 20\AA .

each strip is approximated by a trapezoidal barrier. The effective mass is assumed to be constant in each strip. Under applied bias, the slope of each strip changes according to the external voltage drop across the strip. It is important to choose an appropriate range and width of the strip in order to obtain converged results. In our calculation we have solved it from $-L/2$ to $L/2$ where L is chosen such that the potential profile is constant before applying the external bias. With an N number of strips, the width of each strip is given by $\Delta = L/(N - 1)$. We vary L and N to find the convergence in E_r and Γ values. The dimensionless co-ordinate η takes the form

$$\eta = - \left[\frac{2m[w(z_i)]}{(e\hbar F)^2} \right]^{1/3} (E - V_i(z) - eFz). \quad (40)$$

The wave function for this well is taken as

$$\Psi_E(\eta) = \begin{cases} C_1 Ai(\eta), & z \geq L/2; \\ C_2 Ai(\eta) + D_2 Bi(\eta), & -L/2 + (N - 2)\Delta \leq z \leq -L/2 \\ & + (N - 1)\Delta; \\ C_i Ai(\eta) + D_i Bi(\eta), & -L/2 + (N - i)\Delta \leq z \leq -L/2 \\ & + (N + 1 - i)\Delta; \\ C_{N-1} Ai(\eta) + D_{N-1} Bi(\eta), & -L/2 \leq z \leq -L/2 + \Delta; \\ C_N Ai(\eta) + D_N Bi(\eta), & z < -L/2. \end{cases} \quad (41)$$

The modification of eq. (41) to implement complex Airy function is trivial. In the region $z < -L/2$, the wave function is given by $D_N[Bi(\eta) + jAi(\eta)]$. The boundaries of the small trapezoidals are given as

$$z_i = -\frac{L}{2} + (i - 1)\Delta \quad (42)$$

for $1 \leq i \leq N$. The η at boundaries are calculated as

$$\eta_b^{\pm i} = - \left[\frac{2m_i^+}{(e\hbar F)^2} \right]^{1/3} \{E - V_i^+ - eFz_i\}, \quad (43)$$

$$\eta_a^{\pm i} = - \left[\frac{2m_i^-}{(e\hbar F)^2} \right]^{1/3} \{E - V_i^- - eFz_i\}, \quad (44)$$

where the barrier heights and effective mass in the trapezoidals are taken at the center of each trapezoidal,

$$V_i^{\pm} = V \left(z_i \pm \frac{\Delta}{2} \right), \quad (45)$$

$$m_i^{\pm} = m^* \left[w \left(z_i \pm \frac{\Delta}{2} \right) \right]. \quad (46)$$

In the real Airy function method E_r and Γ are obtained from equations $C_N(E) = 0$ and $\Gamma = 2D_N(E_r)/C'_N(E_r)$ respectively. In the complex Airy function method, they are obtained from the roots of the determinant formed at N boundaries by the current continuity conditions.

As in the previous cases the E_r and Γ are found to be the same in both methods. Our results in table 3 are found to be different from those calculated by Yang *et al* [18]. It is because they have not included the position dependence of the effective mass in the current continuity equation (6b) in their calculations. The effect of the effective mass is quite significant on both E_r and Γ . The quasi-bound energies agree well with our previous Fourier series [15] and finite difference [34] methods. The resonance widths estimated in the present analytic methods do not agree with our previous work based on the finite difference method [34] which solves time-dependent effective mass equations. The barrier interaction and dwelling times arise in the time-dependent methods [35]. On the other hand, the Fourier series technique in the stabilization method is found to give identical results as in the Airy function method since both methods are based on the Breit–Wigner formalism. However, the Airy function method is an order of magnitude faster than the Fourier series method.

Table 3. Ground state energies and mean lifetimes in the single DMQW as shown in figure 3 at different applied electric fields.

F (kV/cm)	$L_d = 10\text{\AA}$		$L_d = 20\text{\AA}$	
	E_r (eV)	Γ (eV)	E_r (eV)	Γ (eV)
50	0.048514	6.862×10^{-23}	0.054363	9.751×10^{-17}
100	0.045554	2.093×10^{-13}	0.050513	4.681×10^{-08}
150	0.040650	1.109×10^{-08}	0.043733	3.458×10^{-05}
200	0.033955	2.306×10^{-06}	0.033438	8.649×10^{-04}
250	0.025346	5.230×10^{-05}	0.019209	5.215×10^{-03}
300	0.014719	3.837×10^{-04}	0.002469	1.504×10^{-02}
350	0.023912	1.502×10^{-03}	-0.015110	2.997×10^{-02}

3. Conclusion

In the present work we have applied the Airy function methods with both real and complex arguments to calculate quasi-bound energies and resonance widths in the single RQW, symmetric DQW and annealing induced DMQW under applied bias. Since these methods are based on the Breit–Wigner formalisms, we find them to give identical results. In reality the tunneling problem is very hard to solve. There is no state-of-art scheme for calculating tunneling time in quantum mechanical problems [35,36]. However, the present scheme is useful for modeling quantum well devices where the quasi-bound energies and mean tunneling lifetimes are important. As mentioned earlier, the inclusion of strain and non-parabolicity effects in this formalism is straight-forward [20]. It is because the strain effect changes the confinement potential whereas the non-parabolicity changes the effective mass, which is also position dependent. The electronic structure calculation in doped quantum wells needs density functional methods. Since the confinement potential, Hartree potential and exchange-correlation potential can be combined as the effective potential in the density functional method, the Airy function methods can also be useful in estimating E_r and Γ quite efficiently in doped wells. We have not shown wave functions for different quantum wells in this paper. However, with known Airy function coefficients this calculation is trivial. The evaluation of the dipole matrix elements for obtaining absorption spectra in the Airy function method has been studied in our earlier work [37]. Further application of the Airy function methods to include hole bands and doping is in progress in our group.

Acknowledgements

The authors are grateful to the referee for inspiring us to find the relation between the real and complex Airy function methods, which has resulted in finding the common Breit–Wigner formula in all methods. The authors also thank S G Mishra and B C Parija for stimulating discussions.

References

- [1] G Bastard, *Wave mechanics applied to semiconductor heterostructures* (Les Editions de physique, 1988)
- [2] Sudhira Panda, *Quantum confined stark effect and optical properties in quantum wells*, Ph.D. thesis (The Hong Kong University, 1998)
- [3] D Ahn and S L Chuang, *IEEE Quantum Electronics* **QE-23**, 2196 (1987)
- [4] W Walukiewicz, *Semiconductor interfaces and microstructures* edited by C F Zhe (World Scientific Publishing Co Pvt. Ltd. 1992) ch. 1
- [5] Paul Harrison, *Quantum wells, wires and dots* (John Wiley and Sons Ltd., 1999)
- [6] E J Austin and M Jaros, *Phys. Rev.* **B31**, 5569 (1985)
- [7] P Enderlein, T Holz and J L Gondar, *Phys. Status Solidi.* **B156**, 259 (1989)
- [8] A K Ghatak, I C Goyal and R L Gallawa, *IEEE J. Quantum Electron.* **26**, 305 (1990)
- [9] D Ahn and S L Chuang, *Phys. Rev.* **B34**, 9034 (1986)
- [10] A K Ghatak, K Thyagarajan and M R Shenoy, *IEEE J. Quantum Electron.* **24**, 1524 (1988)
- [11] F Borondo and J Sánchez-Dehesa, *Phys. Rev.* **B33**, 8758 (1986)
- [12] B Jonsson and S T Eng, *IEEE J. Quantum Electron.* **26**, 2025 (1990)

- [13] K Nakamura, A Shimizu, M Koshiha and K Hayata, *IEEE J. Quantum Electron.* **25**, 889 (1989)
- [14] S Panda, B K Panda, S Fung and C D Beling, *Solid State Commun.* **99**, 299 (1996)
- [15] S Panda, B K Panda and S Fung, *J. Phys. Condens. Matter* **11**, 5293 (1999)
- [16] L D Landau and E M Lifshitz, *Quantum mechanics* (Pergamon Press, 1977)
- [17] J P Peng, H Chen and S X Zhou, *Phys. Rev.* **B43**, 12042 (1991)
- [18] Z Yang, B L Weiss and E H Li, *Superlattices and microstructures* **17**, 177 (1995)
- [19] D C Hutchings, *Appl. Phys. Lett.* **55**, 1082 (1989)
- [20] J P Loehr and M O Manasreh, *Semiconductor quantum wells and superlattices for long-wavelength infrared detectors* (Artech House Inc., Boston, 1993)
- [21] D J BenDaniel and C B Duke, *Phys. Rev.* **152**, 683 (1966)
- [22] *Handbook of mathematical functions*, edited by M Abramowitz and I A Stegun (National Bureau of Standards, Washington DC, 1964) p. 446
- [23] S Adachi, *J. Appl. Phys.* **58**, R1 (1985)
- [24] R J Damburg and V V Kolosov, *J. Phys.* **B9**, 3149 (1976)
- [25] E Luc-Koenig and A Bachelier, *J. Phys.* **B13**, 1743 (1980)
- [26] D M-T Kuo and Y C Chang, *Phys. Rev.* **B60**, 15957 (1999)
- [27] Z Ikonic, V Milanovic and D Tjapkin, *J. Phys.* **C20**, 1147 (1987)
- [28] R L Burden and J D Faires, *Numerical analysis*, 3rd edn. (Prindle, Webers and Schmidt, Boston, 1985)
- [29] R Ferreira and G Bastard, *Rep. Prog. Phys.* **60**, 345 (1997)
- [30] L L Chang and A Koma, *Appl. Phys. Lett.* **29**, 138 (1976)
- [31] T E Schlesinger and T Kuech, *Appl. Phys. Lett.* **49**, 519 (1986)
- [32] K Mukai, M Sugawara and S Yamazaki, *Phys. Rev.* **B50**, 2273 (1993)
- [33] O M Khreis, W P Gillin and K P Homewood, *Phys. Rev.* **B55**, 15813 (1997)
- [34] S Panda, B K Panda, S Fung and C D Beling, *J. Appl. Phys.* **80**, 1532 (1996)
- [35] R Landauer and Th Martin, *Rev. Mod. Phys.* **66**, 217 (1994)
- [36] N Yamada, *Phys. Rev. Lett.* **83**, 3350 (1999)
- [37] S Panda, B K Panda, S Fung and C D Beling, *Phys. Status Solidi.* **B194**, 547 (1996)